

See discussions, stats, and author profiles for this publication at: <https://www.researchgate.net/publication/228690476>

# The Influence of Carboxyl Groups on the Photoluminescence of Mercaptocarboxylic Acid-Stabilized CdTe Nanoparticles

ARTICLE in THE JOURNAL OF PHYSICAL CHEMISTRY B · JANUARY 2003

Impact Factor: 3.3 · DOI: 10.1021/jp025910c

CITATIONS

457

READS

191

## 4 AUTHORS, INCLUDING:



**Hao Zhang**

North Sichuan Medical College

263 PUBLICATIONS 4,574 CITATIONS

SEE PROFILE



**Yang Bai**

Iowa State University

446 PUBLICATIONS 9,298 CITATIONS

SEE PROFILE



**Mingyuan Gao**

Chinese Academy of Sciences

108 PUBLICATIONS 6,362 CITATIONS

SEE PROFILE

## ARTICLES

**The Influence of Carboxyl Groups on the Photoluminescence of Mercaptocarboxylic Acid-Stabilized CdTe Nanoparticles****Hao Zhang, Zhen Zhou, and Bai Yang\****Key Lab of Supramolecular Structure & Materials; Department of Chemistry, Jilin University, Changchun, 130023, P. R. China***Mingyuan Gao\****Institute of Chemistry, Chinese Academy of Sciences, Beijing 100080, P. R. China**Received: April 8, 2002; In Final Form: September 12, 2002*

The CdTe nanoparticles were prepared in aqueous solution using different mercaptocarboxylic acids such as 3-mercaptopropionic acid (MPA) and thioglycolic acid (TGA) as stabilizing agents following the synthetic route described in ref 9. The pH-dependent photoluminescence (PL) of MPA- and TGA-stabilized CdTe nanoparticles was systematically investigated before and after addition of poly(acrylic acid) (PAA) into the CdTe solutions. Experimental results reveal that lowering the pH can increase the PL efficiency of both MPA- and TGA-stabilized CdTe. Moreover, the PL of the CdTe can further be increased in the presence of PAA in low pH range. X-ray photoelectron spectroscopy (XPS) was employed to investigate the interaction between the carboxyl groups from PAA and CdTe nanoparticles which were assembled in polymer matrix by a layer-by-layer self-assembly method to exclude interference from other species in CdTe solutions. XPS results demonstrate that the S/Te ratio of CdTe particles decreases after the addition of PAA, which strongly suggests that PAA can strongly interact with CdTe nanoparticles via the coordination between carboxyl groups and cadmium ions on the particle surface. As a result, the PL efficiency of the mercaptocarboxylic acid-stabilized CdTe nanoparticles is enhanced in acidic range.

**1. Introduction**

Exploring novel materials based on semiconductor nanoparticles has become one of the most attractive areas of current research.<sup>1–4</sup> Due to quantum confinement effects, semiconductor nanoparticles exhibit unique physical and chemical properties distinctly different from their corresponding individual molecules or bulk materials.<sup>5,6</sup> Over the past two decades, significant progress has been achieved in controlling the size and surface of wet-chemically synthesized semiconductor nanoparticles.<sup>7–17</sup> Water-soluble semiconductor nanoparticles with high photoluminescence (PL) quantum efficiency have shown great potentials in photonic crystals,<sup>18,19</sup> thin-film light-emitting devices,<sup>20–22</sup> and especially biological labels.<sup>23,24</sup> Water-soluble semiconductor nanoparticles with high PL efficiency can be obtained mainly by two different ways. The first way is to replace the surface-capping molecules on particles prepared by TOPO method with water-soluble thiols or silica shell.<sup>23–31</sup> The second way is to directly synthesize semiconductor nanoparticles in aqueous solutions using water-soluble thiols as stabilizing agents.<sup>32–39</sup> In these two approaches, the water-soluble thiols play an important role and contribute greatly to the stability and the functionality of the resulting nanoparticles.<sup>9,23,24,27–31,33,34</sup> In addition, different choices of water-soluble thiols also

critically determine the PL efficiency due to the difference in the resulting particle surface structures.<sup>9,25,37</sup> Therefore, studies of surface structure of thiol-stabilized nanoparticles continue to be of great importance in controlling the optical properties of nanoparticle materials.<sup>23,40,41</sup>

Experimentally, pH-dependent PL is observed from the colloidal CdTe nanoparticles stabilized by mercaptocarboxylic acids.<sup>9</sup> One possible explanation is the formation of annulus complexes forming in acidic pH range from cadmium ions and mercaptocarboxylic acids around the CdTe particle core, which provides better surface passivation at low pH to the CdTe nanoparticles.<sup>9,19,33,36,37</sup> However, more experiments are still required in order to understand the influence of the surface structure on the PL efficiency of the CdTe nanoparticles, for example whether the coordination between the carboxyl group from the particle surface-capping mercaptocarboxylic acid and cadmium ions on the particle surface can form at low pH and change the CdTe particle surface properties. In this paper, we report CdTe nanoparticles prepared in the presence of two different mercaptocarboxylic acids such as 3-mercaptopropionic acid and thioglycolic acid. The impact of the carboxyl group from the mercaptocarboxylic acids on the PL efficiency is investigated. The interaction between the carboxyl groups and the particle surface is further studied by adding polycarboxylic acid into the mercaptocarboxylic acid-stabilized CdTe solutions. Combining with X-ray photoelectron spectroscopic results, the

\* Authors to whom correspondence should be addressed. E-mails: yangbai@jlu.edu.cn, gaomy@infoc3.icas.ac.cn.

particle surface composition and the correlation between the particle surface structure and particle PL efficiency are discussed.

## 2. Experimental Section

3-Mercaptopropionic acid (MPA) (Aldrich, 99+%), thiolglycolic acid (TGA) (Aldrich, 97+%), poly(acrylic acid) (PAA) (Aldrich,  $M_V$  ca. 450 000), poly(methacrylic acid, sodium salt) (PMAA) (Aldrich,  $M_W$  ca. 9500, 30 wt % solution in water), poly(diallyldimethylammonium chloride) (PDDA) (Aldrich,  $M_W$  ca. 100 000–200 000, 20 wt % solution in water),  $\text{CdCl}_2$  (99+%),  $\text{NaBH}_4$  (99%), and tellurium powder (Aldrich, –200 mesh, 99.8%) are commercially available products.

**a. Preparation of Sodium Hydrogen Telluride.** By a molar ratio of 2:1, sodium borohydride was used to react with tellurium in water to produce sodium hydrogen telluride ( $\text{NaHTe}$ ).<sup>33</sup> Briefly, 80 mg of sodium borohydride was transferred to a small flask; then 1 mL of ultrapure water was added. After 127.5 mg of tellurium powder was added in the flask, the reacting system was cooled by ice. During the reaction, a small outlet connected to the flask was kept open to discharge the pressure from the resulting hydrogen. After approximately 8 h, the black tellurium powder disappeared and sodium tetraborate white precipitation appeared on the bottom of the flask instead. The resulting  $\text{NaHTe}$  in clear supernatant was separated and used in the preparation of CdTe particles.

**b. Preparation of CdTe Nanoparticles.** A series of aqueous colloidal CdTe solutions were prepared by adding freshly prepared  $\text{NaHTe}$  solution to  $1.25 \times 10^{-3}$  N  $\text{N}_2$ -saturated  $\text{CdCl}_2$  solutions at pH 9.0 in the presence of mercaptocarboxylic acids as a stabilizing agent.<sup>33</sup> The molar ratio of  $\text{Cd}^{2+}$ /stabilizer/ $\text{HTe}^-$  was fixed at 1:2.4:0.5. The resulting mixture was then subjected to a reflux that controlled the growth of the CdTe nanocrystals. In brief, CdTe particles with their size ranging from 2.8 to 4.0 nm were obtained. HCl and mercaptocarboxylic acid were used in the investigation of the pH-dependent photoluminescence of the CdTe nanoparticles obtained.

**c. Preparation of CdTe Solutions Containing PAA.** 2.9 nm CdTe nanoparticles were chosen to prepare the PAA-containing CdTe solution. The concentration of carboxyl groups from PAA was controlled the same as that from mercaptocarboxylic acid in the CdTe solution (standard PAA concentration). Typically, 3 mL of 0.1 N PAA aqueous solution (pH 9.0) was added to 100 mL of CdTe stock solution.

**d. Fabrication of CdTe Nanoparticle/PDDA Multilayer Films.** Freshly cleaned substrates (quartz slides and single-crystal silicon wafer) were first covered by one thin layer of PDDA by immersing the substrates into the PDDA solution (0.9 vol %). Then the PDDA-modified substrates were alternately dipped into CdTe aqueous solution and the PDDA solution for 20 min, respectively, interrupted by water-washing and  $\text{N}_2$ -drying processes after the deposition of each layer of CdTe/PDDA.

**e. Characterization.** UV–Vis absorption spectra were obtained by using a Shimadzu 3100 UV–Vis–near-IR spectrophotometer. Fluorescence experiments were performed with the help of a Shimadzu RF-5301 PC spectrofluorimeter. All optical measurements were performed at room temperature under ambient conditions.

X-ray photoelectron spectroscopy (XPS) was investigated by using a VG ESCALAB MK II spectrometer with a Mg K $\alpha$  excitation (1253.6 eV). Binding energy calibration was based on C 1s at 284.6 eV. Transmission electron micrographs (TEM) and selected area electron diffraction (SAED) were recorded

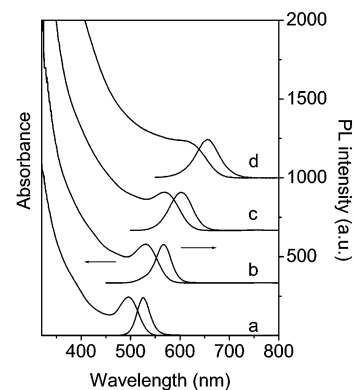


**Figure 1.** UV-Vis absorption and photoluminescence spectra of differently sized MPA-stabilized CdTe nanoparticles. Photoluminescence spectra were recorded with an excitation at 400 nm. The average diameters of the nanoparticles are (a) 2.8 nm (QY  $\sim$  18%), (b) 3.3 nm (QY  $\sim$  38%), (c) 3.6 nm (QY  $\sim$  17%), and (d) 4.0 nm (QY  $\sim$  2%), which were estimated from their corresponding excitonic absorption peaks.

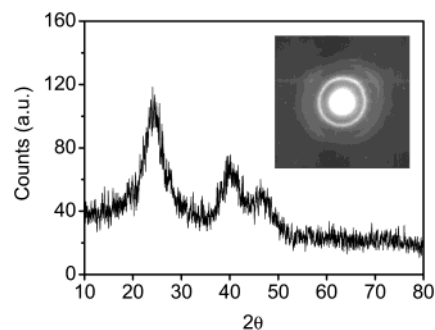


**Figure 2.** XRD and SAED patterns recorded from MPA-stabilized CdTe nanoparticles. The average diameters of this sample are 2.9 nm.

by a JEOL-2010 electron microscope operating at 200 kV. X-ray powder diffraction (XRD) was carried out using a Siemens D5005 diffractometer.

## 3. Results and Discussion

**a. Characterization of Mercaptocarboxylic Acid-Stabilized CdTe Nanoparticles.** Figure 1 presents typical evolutions of both absorption and photoluminescence spectra of MPA-stabilized CdTe nanoparticles as a function of particle size. The average particle size of samples shown in Figure 1 was derived from the 1s–1s electronic transition in the absorption spectra based on a theoretical model from a previous report.<sup>42</sup> The size and size distribution of the CdTe nanoparticles were further confirmed by TEM. Under TEM, the CdTe appear as spherical particles with crystalline structures. On average, the particle size distribution is around 15%.

Both absorption and PL spectra shown in Figure 1 exhibit “quantum size effects”. The excitonic peak position in absorption shifts from 494 to 611 nm when the particle size increases from 2.8 to 4.0 nm by reflux. In the meantime, PL peak position shifts from 522 to 655 nm. The relative PL quantum yields (QY) of four different CdTe samples with particle diameters of 2.8, 3.3, 3.6, and 4.0 nm are estimated to be 18%, 38%, 17%, and 2%, respectively, using Rhodamine 6G as PL reference. CdTe nanoparticles (3.6 and 4.0 nm) were obtained by a size selective precipitation procedure using 2-propanol as bad solvent to narrow the particle size distribution.

The XRD and SAED of 2.9 nm CdTe nanoparticles are presented in Figure 2. The SAED pattern appears as broad diffuse rings due to the small particle size. The powder XRD

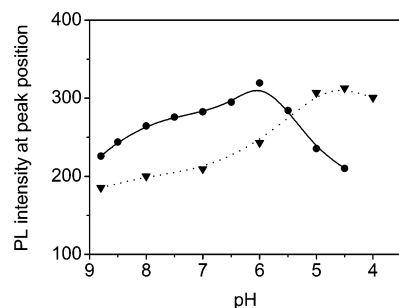


**Figure 3.** The peak fluorescence intensity of CdTe nanoparticles versus pH values. MPA-stabilized CdTe nanoparticles (solid), and TGA-stabilized CdTe nanoparticles (dot).

**TABLE 1: The  $pK_{\text{COOH}}$  and  $pK_{\text{SH}}$  of a Series of Compounds Containing Carboxyl Groups**

chemicals	$pK_{\text{SH}}$	$pK_{\text{COOH}}$
TGA	10.05	3.53
MPA	10.20	4.32
PAA		4.75
PMAA		5.65

profile of the nanoparticles shows broad peaks typical for nanocrystals. The lattice parameters derived from SAED and XRD measurements for MPA-stabilized CdTe nanoparticles fit to the cubic zinc blende structure of bulk CdTe crystal.<sup>39</sup> Therefore, the cubic crystalline structure is adopted to estimate the surface coverage of sulfur for any given S/Te ratio.

**b. The pH-Dependent PL of Mercaptocarboxylic Acid-Stabilized CdTe Nanoparticles.** To use mercaptocarboxylic acid as a stabilizer in the syntheses of CdTe nanoparticles is very important to gain both the stability and the functionality of the resulting particles.<sup>9,23,27–31,33–37</sup> Similar to the thioglycolic acid-stabilized CdTe,<sup>9</sup> the 3-mercaptopropionic acid-stabilized CdTe nanoparticles also show pH-dependent photoluminescence. Figure 3 presents fluorescent intensity of CdTe-MPA and CdTe-TGA vs pH value. Solutions of 0.1 N MPA and TGA were used to decrease the pH of the corresponding CdTe solutions. The fluorescent intensity of the TGA-stabilized CdTe increases gradually with the decrease of pH. Then it stops increasing until the pH of solution reaches 4.5. Similarly, the fluorescent intensity of the MPA-stabilized CdTe increases until the pH arrives at 6.0, then it decreases drastically upon further decrease of pH. Comparing MPA with TGA, the main difference in chemistry is  $pK_{\text{COOH}}$  rather than  $pK_{\text{SH}}$  as shown in Table 1. Since MPA has a larger  $pK_{\text{COOH}}$ , the required pH value to convert carboxylate into carboxylic acid is higher. The pH-dependent PL in Figure 3 clearly tells that the MPA-stabilized CdTe reaches its PL maximum at a higher pH than TGA-stabilized CdTe. Therefore, it is reasonable to partly attribute the pH-dependent PL behaviors of MPA- and TGA-stabilized CdTe to the protonation of carboxylate groups from particle surface-binding thiols. A previous report has proved the existence of a secondary coordination between the carboxyl oxygen from  $\text{Cd}(\text{SCH}_2\text{COOCH}_2\text{CH}_3)_2$  and primary thiol-binding cadmium.<sup>43</sup> It can then be deduced that a secondary coordination between the carbonyl O atom of free acid and the Cd atom at the CdTe particle surface exists, which in return provides better surface passivation and consequently higher PL efficiency. In fact, the PL of CdTe is not solely determined by the interaction between carboxyl groups from mercaptocarboxylic acids and particle surface in the acidic range. Lowering the pH value also changes the CdTe surface complexes formed by excess of mercaptocarboxylic acids and cadmium ions which remain in the CdTe solutions. According to previous reports, complexes of mer-

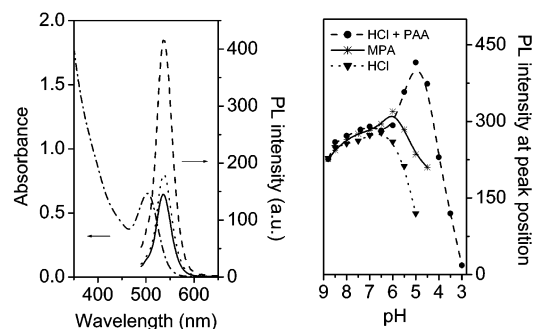


**Figure 4.** Left panel: Absorption and fluorescence spectra of MPA-stabilized CdTe solutions with a PAA concentration of  $3 \times 10^{-3}$  N (referring to carboxylic acid group). Only one absorption spectrum (dash dot) is presented since it remains unchanged at different pH values. Fluorescence spectra recorded at different pH values, 9.0 (solid), 6.0 (dot), and 5.0 (dash). Right panel: Peak fluorescence intensity of MPA-stabilized CdTe solutions versus pH values treated by using HCl (dot), MPA (solid), and HCl in the presence of PAA (dash).

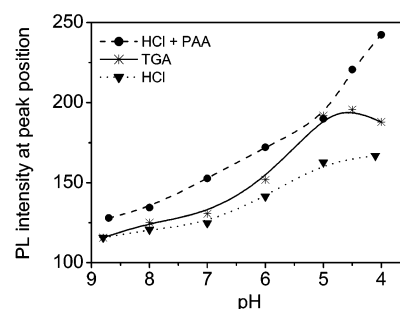


**Figure 5.** Peak fluorescence intensity of TGA-stabilized CdTe solutions versus pH values treated by using HCl (dot), TGA (solid), and HCl in the presence of PAA (dash).

captocarboxylic acid and cadmium ions contribute to the PL enhancement and the stability of the CdTe solution at low pH.<sup>9,36,37</sup> The influences of  $\text{Cd}^{2+}$ , thiols, as well as  $\text{Cd}^{2+}$ –thiol complexes have systematically been investigated;<sup>9</sup> however the impact of carboxyl groups on the PL is still unknown.

**c. The Influence of Carboxyl Groups on the PL of CdTe Nanoparticles.** To avoid the interference of thiol groups from mercaptocarboxylic acids, PAA was chosen to check the PL enhancement effect solely originated from carboxylic acids. Figure 4 shows the influence of PAA on the pH-dependent PL of MPA-stabilized CdTe nanoparticles. Diluted HCl and MPA solutions were used to tune the pH of the CdTe solution to the acidic range. Upon addition of 3 mL 0.1 N (referring to carboxylic acid group) PAA into 100 mL of CdTe stock solution in the basic range, no obvious PL enhancement was observed. The PL intensity increases gradually with the decrease of pH until the pH becomes 6.0, then it rises dramatically. During this process, the absorption spectra of the CdTe solution remains nearly unchanged, providing evidence that no particle growth occurs. The PL intensity reaches its maximum at pH 5.0, and then decays rapidly upon further decrease of pH. Compared with the maximum PL intensity achieved in the absence of PAA, the PL intensity obtained in the presence of PAA is increased by a factor of 1.5. Similar pH-dependent PL is also observed from the TGA-stabilized CdTe in the presence of PAA (Figure 5).

Along with the decrease of pH, a red-shifted PL was observed from the MPA-stabilized CdTe in the low pH range. The red-shift in PL is attributed to an additional sulfuration reaction taking place on the CdTe surface during the decrease of the pH value.<sup>9</sup> It is also demonstrated that the red-shift greatly depends



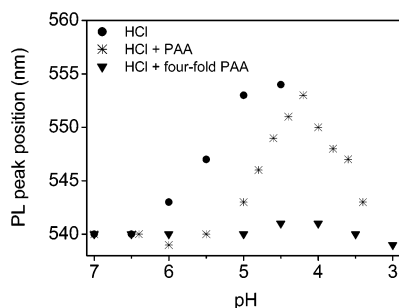


**Figure 6.** Fluorescence peak position of MPA-stabilized CdTe solutions versus pH values obtained by using HCl (circle), HCl with a PAA concentration of  $3 \times 10^{-3}$  N (snow), HCl with a PAA concentration of  $1.2 \times 10^{-2}$  N (triangle).

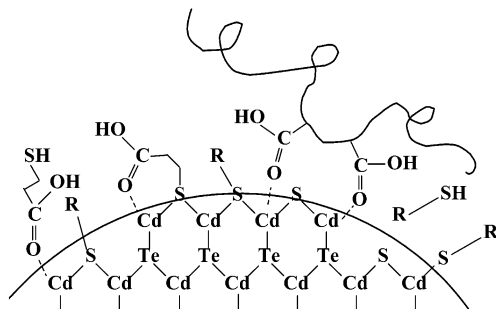


**Figure 7.** Schematic illustration of the surface structure of CdTe nanoparticles modified with MPA and PAA. The coil represents the PAA alkyl chain. R represents a carboxylic acid group. The coordination between the carbonyl oxygen and cadmium on the particle surface is represented as dot line. The naked sulfur species in the particle resulted from the decomposition of thiols.

on the concentration of PAA (Figure 6). In the absence of PAA, the PL exhibits a gradual red-shift up to 14 nm before precipitation of CdTe appears at pH 4.5. In contrast, there is no precipitation observed in the same pH range for the PAA–CdTe system. Upon further decrease of pH, the fluorescence peak shifts back nearly to the original value in the presence of PAA. It is also observed that higher concentration of PAA offers better stability to the CdTe solution and gives rise to a much smaller PL shift as shown in Figure 6. This result reveals that PAA can effectively stabilize the CdTe particles in acidic range apart from its contribution to the PL enhancement effect due to the strong interaction between PAA and the CdTe particles.

On the basis of the above-mentioned results, it is reasonable to conclude that the carboxyl acid groups can interact with the CdTe particles in the acidic range, which contributes to the PL enhancement in addition to the contribution from the  $\text{Cd}^{2+}$ –mercaptocarboxylic acid complexes. In general, the cadmium ions on the particle surface can coordinate with both  $-\text{SH}$  and  $-\text{COOH}$  groups.<sup>43</sup> In comparison with carboxyls from the mercaptocarboxylic acid, the PAA carboxyl group has a stronger coordinative ability with  $\text{Cd}^{2+}$  on the particle surface due to the multiple binding sites from each single PAA chain.<sup>44</sup> The particle surface structure is proposed in Figure 7. The PAA chains wrap around the fluorescent CdTe nanoparticles via the interaction between carboxyl and cadmium, which will provide a stabilizing effect to the CdTe.<sup>45,46</sup> Such a structure has been proposed for poly(ethylene glycol) oligomer-supported CdS nanoclusters and CdSe nanocrystals modified by dendrons.<sup>31,47</sup>

One essential question on the validity of our proposed model is whether the coordination between the PAA carboxyls and nanoparticles is strong enough to complex PAA with CdTe. FTIR measurements were performed to demonstrate the strong interaction between the CdTe nanoparticles and PAA. Our

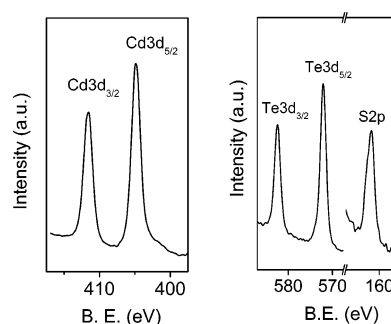


**Figure 8.** X-ray photoelectron spectra from {CdTe/polyelectrolyte}<sup>3</sup> layer thin films, assembled layer-by-layer on a clean single-crystal silicon substrate precoated with PDPA, then CdTe. (a) Cd 3d spectrum, and (b) Te 3d, S 2p spectrum.

**TABLE 2: The Calculated Number of S Atoms per nm<sup>2</sup> of CdTe Particle Surface. Cubic Zinc Blende Model Is Employed for 2.9 nm CdTe Nanoparticles. The S/Te Ratios Used in the Calculation Were Obtained by XPS Measurements**

pH	number of S atoms per nm <sup>2</sup> of particle surface			
	MPA-stabilized CdTe		TGA-stabilized CdTe	
	in the absence of PAA	in the presence of PAA	in the absence of PAA	in the presence of PAA
9.0	5.4	5.5	4.8	5.3
6.0	10.2	6.0	8.1	6.5
5.0	8.5	5.9	10.8	7.9

preliminary results show a shift in the carboxyl stretching vibration band after PAA is mixed with CdTe in solution. However, it is difficult to quantitatively characterize the IR shift since absorptions of MPA carboxyls and PAA carboxyls are difficult to clearly differentiate. Another problem in investigating the existence of the association between PAA and CdTe nanoparticles is how to maintain the surface structure of nanoparticles and exclude interference from small molecules in solution. To solve this problem, a layer-by-layer self-assembly method was adopted to embed CdTe nanoparticles in polymer matrix utilizing columbic interactions between negatively charged CdTe and positively charged PDPA.<sup>33</sup> The elemental composition of the CdTe/PDPA multilayer films was analyzed by XPS.<sup>48</sup> The appearance of a characteristic Cd 3d<sub>5/2</sub> peak at 404.5 eV, S 2p peak at 161.8 eV, and Te 3d<sub>5/2</sub> peak at 571.9 eV shown in Figure 8 confirms the existence of cadmium, tellurium, and sulfur species in the film.<sup>49</sup> In addition, XPS data from Figure 8 also allow the determination of atomic ratios between S and Te from the particles which were originally kept in solutions of different pH. The S/Te ratio is very important for studying the change of surface-binding thiols upon addition of PAA. Using a cubic zinc blende model, the surface coverage of thiols on the CdTe surface is estimated. As shown in Table 2, the maximum number of surface-binding S on MPA-stabilized CdTe nanoparticles is located around pH 6.0 in the absence of PAA, whereas the number of surface-binding S on TGA-stabilized CdTe nanoparticles keeps increasing in the absence of PAA until the pH arrives at 5.0. This result further confirms the previous proposed mechanism on the PL enhancement caused by the formation of  $\text{Cd}^{2+}$ –mercaptocarboxylic acid complexes on the particle surface at low pH and also explains the pH-dependent PL of MPA-stabilized CdTe in the absence of PAA. However, in the presence of PAA the surface coverage of the S atom remains nearly unchanged in the investigated pH range of 9.0–5.0 for the MPA-stabilized CdTe, which suggests that the pH-dependent interaction between PAA and the CdTe particle critically determines the PL of the CdTe nanoparticles.

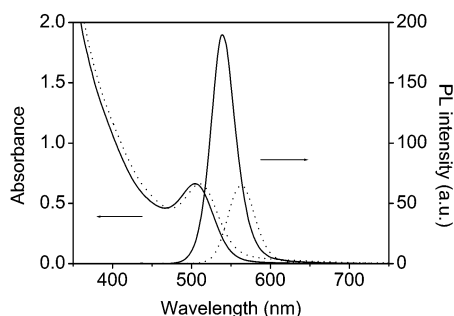


**Figure 9.** Absorption and fluorescence spectra of purified MPA-stabilized CdTe solutions at pH 5.1. CdTe solutions in the absence of PAA (dot), and CdTe solutions in the presence of PAA (solid).

In addition, generally smaller S surface coverage of the CdTe–PAA system than that of the pure CdTe system indicates that some of the surface-binding thiols are replaced by PAA, which further proves the strong interaction between PAA and CdTe nanoparticles (Table 2). The following experiment also provides more evidence on this interaction. To exclude possible interference from the excess MPA and  $\text{Cd}^{2+}$  in CdTe stock solutions, the MPA-stabilized CdTe nanoparticles were purified by precipitation in 2-propanol and then redissolved in water. As shown in Figure 9, the PL intensity of this purified CdTe particle solution become less pronounced at pH 5.1 compared to that given in Figure 3. In the absence of excess MPA and  $\text{Cd}^{2+}$ , the PL intensity decrease with the decrease of pH as a result of the deconstruction of the complexes annulus due to the protonation of the surface-binding thiolates. However, the PL of the purified CdTe solution can still be enhanced by a factor of 2 in the presence of PAA after the pH is tuned to 5.1. Since there is no excess mercaptocarboxylic acid existing in the CdTe solution, it can be concluded that the observed PL enhancement purely originates from the combination between nanoparticles and carboxyl groups. This result further supports our model proposed in Figure 7.

#### d. Other Chemicals Terminated with Carboxyl Groups.

When poly(methacrylic acid) (PMAA) is adopted instead of PAA, no PL enhancement will be observed. This can be explained by the spatial hindering effect of the methyl group preventing the carboxylic acid groups from binding the Cd ions on the particle surface.<sup>50</sup> It should be mentioned that no direct effect from the molecular weight of polycarboxylic acid was observed on the PL enhancement effect.

## Conclusions

Systematic pH-dependent photoluminescence and XPS studies have demonstrated that carboxyl groups have a great influence on both photoluminescence and stability of the mercaptocarboxylic acid-stabilized CdTe nanoparticles. The coordination between the carboxyl groups and cadmium ions can effectively improve the PL efficiency of the CdTe nanoparticles. But this enhancement effect is only observed in a certain acidic range, which suggests that the interaction between carboxyl groups and the CdTe particle surface can effectively diminish the nonradiative channel for electron–hole recombination. However, two important questions remain open: (1) the details of pH-dependent chemical interaction between the carboxyl groups and cadmium ions on the particle surface, and (2) physical explanations of the PL enhancement effect involving PAA. Nonetheless, the PL enhancement effect from the carboxyl groups will provide useful instructions on chemical syntheses of highly fluorescent CdTe in aqueous solution.

**Acknowledgment.** This work was supported by National Natural Science Foundation of China (Nos. 29925412, 200340062). M.Y.G. acknowledges the Chinese Academy of Sciences for financial support through “Hundred-talent Program”.

## References and Notes

- (1) Weller, H. *Angew. Chem., Int. Ed. Engl.* **1993**, *32*, 41–53.
- (2) Alivisatos, A. P. *Science* **1996**, *271*, 933–937.
- (3) Fendler, J. H. *Chem. Mater.* **2001**, *13*, 3196–3210.
- (4) Klimov, V. I.; Mikhailovsky, A. A.; Xu, S.; Malko, A.; Hollingsworth, J. A.; Leatherdale, C. A.; Eisler, H.-J.; Bawendi, M. G. *Science* **2000**, *290*, 314–317.
- (5) Nirmal, M.; Brus, L. *Acc. Chem. Res.* **1999**, *32*, 407–414.
- (6) Kagan, C. R.; Murray, C. B.; Bawendi, M. G. *Phys. Rev. B* **1996**, *54*, 8633–8643.
- (7) Peng, X.; Manna, L.; Yang, W.; Wickham, J.; Scher, E.; Kadavani, A.; Alivisatos, A. P. *Nature* **2000**, *404*, 59–61.
- (8) Pantes, V. F.; Krishnan, K. M.; Alivisatos, A. P. *Science* **2001**, *291*, 2115–2117.
- (9) Gao, M. Y.; Kirstein, S.; Möhwald, H.; Rogach, A. L.; Kornowski, A.; Eychmüller, A.; Weller, H. *J. Phys. Chem. B* **1998**, *102*, 8360–8363.
- (10) Peng, Z. A.; Peng, X. *J. Am. Chem. Soc.* **2001**, *123*, 183–184.
- (11) Qu, L.; Peng, Z. A.; Peng, X. *Nano Lett.* **2001**, *1*, 333–337.
- (12) Gautam, U. K.; Rajamathi, M.; Meldrum, F.; Morgan, P.; Seshadri, R. *Chem. Commun.* **2001**, 629–630.
- (13) Cao, Y. W.; Banin, U. *J. Am. Chem. Soc.* **2000**, *122*, 9692–9702.
- (14) Hao, E.; Sun, H.; Zhou, Z.; Liu, J.; Yang, B.; Shen, J. C. *Chem. Mater.* **1999**, *11*, 3096–3102.
- (15) Dabbousi, B. O.; Rodriguez-Viejo, J.; Mikulec, F. V.; Heine, J. R.; Mattoussi, H.; Ober, R.; Jensen, K. F.; Bawendi, M. G. *J. Phys. Chem. B* **1997**, *101*, 9463–9475.
- (16) Hines, M. A.; Guyot-Sionnest, P. *J. Phys. Chem. B* **1998**, *102*, 3655–3657.
- (17) Ludolph, B.; Malik, M. A.; O'Brien, P.; Revaprasadu, N. *Chem. Commun.* **1998**, 1849–1850.
- (18) Rogach, A. L.; Kotov, N. A.; Koktysh, D. S.; Ostrander, J. W.; Ragoisha, G. A. *Chem. Mater.* **2000**, *12*, 2721–2726.
- (19) Rogach, A. L.; Sussha, A.; Caruso, F.; Sukhorukov, G.; Kornowski, A.; Kershaw, S.; Möhwald, H.; Eychmüller, A.; Weller, H. *Adv. Mater.* **2000**, *12*, 333–337.
- (20) Colvin, V. L.; Schlamp, M. C.; Alivisatos, A. P. *Nature* **1994**, *370*, 354–357.
- (21) Gao, M. Y.; Richter, B.; Kirstein, S.; Möhwald, H. *J. Phys. Chem. B* **1998**, *102*, 4096–4103.
- (22) Mamedov, A. A.; Belov, A.; Giersig, M.; Mamedov, N. N.; Kotov, N. A. *J. Am. Chem. Soc.* **2001**, *123*, 7738–7739.
- (23) Chan, W. C. W.; Nie, S. *Science* **1998**, *281*, 2016–2018.
- (24) Jr, M. B.; Moronne, M.; Gin, P.; Weiss, S.; Alivisatos, A. P. *Science* **1998**, *281*, 2013–2016.
- (25) Rogach, A. L.; Nagesha, D.; Ostrander, J. W.; Giersig, M.; Kotov, N. A. *Chem. Mater.* **2000**, *12*, 2676–2685.
- (26) Gerion, D.; Pinaud, F.; Williams, S. C.; Parak, W. J.; Zanchet, D.; Weiss, S.; Alivisatos, A. P. *J. Phys. Chem. B* **2001**, *105*, 8861–8871.
- (27) Mattoussi, H.; Mauro, J. M.; Goldman, E. R.; Anderson, G. P.; Sundar, V. C.; Mikulec, F. V.; Bawendi, M. G. *J. Am. Chem. Soc.* **2000**, *122*, 12142–12150.
- (28) Aldana, J.; Wang, Y. A.; Peng, X. *J. Am. Chem. Soc.* **2001**, *123*, 8844–8850.
- (29) Willard, D. M.; Carillo, L. L.; Jung, J.; Orden, A. V. *Nano Lett.* **2001**, *1*, 469–474.
- (30) Mitchell, G. P.; Mirkin, C. A.; Letsinger, R. L. *J. Am. Chem. Soc.* **1999**, *121*, 8122–8123.
- (31) Wang, Y. A.; Li, J. J.; Chen, H.; Peng, X. *J. Am. Chem. Soc.* **2002**, *124*, 2293–2298.
- (32) Sun, Y. P.; Hao, E.; Zhang, X.; Yang, B.; Gao, M. Y.; Shen, J. C. *Chem. Commun.* **1996**, 2381–2382.
- (33) Hao, E.; Zhang, H.; Yang, B.; Ren, H.; Shen, J. C. *J. Colloid Interface Sci.* **2001**, *238*, 285–290.
- (34) Lawless, D.; Kapoor, S.; Meisel, D. *J. Phys. Chem.* **1995**, *99*, 10329–10335.
- (35) Tang, Z.; Kotov, N. A.; Giersig, M. *Science* **2002**, *297*, 237–240.
- (36) Talapin, D. V.; Rogach, A. L.; Shevchenko, E. V.; Kornowski, A.; Haase, M.; Weller, H. *J. Am. Chem. Soc.* **2002**, *124*, 5782–5790.
- (37) Gaponik, N.; Talapin, D. V.; Rogach, A. L.; Hoppe, K.; Shevchenko, E. V.; Kornowski, A.; Eychmüller, A.; Weller, H. *J. Phys. Chem. B* **2002**, *106*, 7177–7185.
- (38) Rogach, A. L.; Kornowski, A.; Gao, M. Y.; Eychmüller, A.; Weller, H. *J. Phys. Chem. B* **1999**, *103*, 3065–3069.
- (39) Rogach, A. L.; Katsikas, L.; Kornowski, A.; Su, D.; Eychmüller, A.; Weller, H. *Ber. Bunsen-Ges. Phys. Chem.* **1996**, *100*, 177–1778.

- (40) Chen, C. C.; Yet, C. P.; Wang, H. N.; Chao, C. Y. *Langmuir* **1999**, *15*, 6845–6850.
- (41) Maye, M. M.; Luo, J.; Han, L.; Zhong, C. J. *Nano Lett.* **2001**, *1*, 575–579.
- (42) Rajh, T.; Mićić, O. I.; Nozik, A. J. *J. Phys. Chem.* **1993**, *97*, 11999–12003.
- (43) Dance, I. G.; Scudder, M. L.; Secomb, R. *Inorg. Chem.* **1983**, *22*, 1794–1797.
- (44) Benegas, J. C.; Cleven, R. F. M. J.; van den Hoop, M. A. G. T. *Anal. Chim. Acta* **1998**, *369*, 109–114.
- (45) Nickel, A. L.; Seker, F.; Ziemer, B. P.; Ellis, A. B. *Chem. Mater.* **2001**, *13*, 1391–1397.
- (46) Bonapasta, A. A.; Buda, F.; Colombet, P. *Chem. Mater.* **2001**, *13*, 64–70.
- (47) Bekiari, V.; Lianos, P. *Langmuir* **2000**, *16*, 3561–3563.
- (48) Katari, J. E. B.; Colvin, V. L.; Alivisatos, A. P. *J. Phys. Chem.* **1994**, *98*, 4109–4117.
- (49) Vesely, C. J.; Langer, D. W. *Phys. Rev. B* **1971**, *4*, 451–462.
- (50) Porasso, R. D.; Benegas, J. C.; van den Hoop, M. A. G. T. *J. Phys. Chem. B* **1999**, *103*, 2361–2365.